

UNCLASSIFIED

AD 433737

DEFENSE DOCUMENTATION CENTER

FOR

SCIENTIFIC AND TECHNICAL INFORMATION

CAMERON STATION, ALEXANDRIA, VIRGINIA



UNCLASSIFIED

NOTICE: When government or other drawings, specifications or other data are used for any purpose other than in connection with a definitely related government procurement operation, the U. S. Government thereby incurs no responsibility, nor any obligation whatsoever; and the fact that the Government may have formulated, furnished, or in any way supplied the said drawings, specifications, or other data is not to be regarded by implication or otherwise as in any manner licensing the holder or any other person or corporation, or conveying any rights or permission to manufacture, use or sell any patented invention that may in any way be related thereto.

64-11

433737

ARL 64-27

RESEARCH ON HYPERSONIC FLOW

CATALOGED BY DDC

AS /

H. F. WALDRON
G. E. WITTLIFF
M. R. WILSON

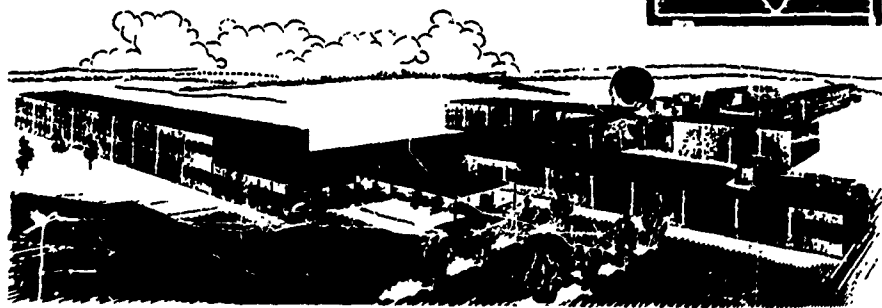
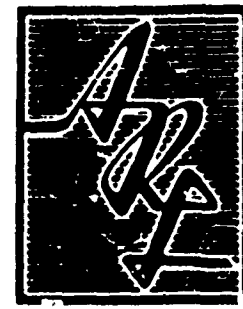
CORNELL AERONAUTICAL LABORATORY, INC.
BUFFALO, NEW YORK

FEBRUARY 1964

1964

433737

AEROSPACE RESEARCH LABORATORIES
OFFICE OF AEROSPACE RESEARCH
UNITED STATES AIR FORCE



NOTICES

When Government drawings, specifications, or other data are used for any purpose other than in connection with a definitely related Government procurement operation, the United States Government thereby incurs no responsibility nor any obligation whatsoever; and the fact that the Government may have formulated, furnished, or in any way supplied the said drawings, specifications, or other data, is not to be regarded by implication or otherwise as in any manner licensing the holder or any other person or corporation, or conveying any rights or permission to manufacture, use, or sell any patented invention that may in any way be related thereto.

.....

Qualified requesters may obtain copies of this report from the Defense Documentation Center, (DDC), Cameron Station, Alexandria, Virginia.

.....

This report has been released to the Office of Technical Services, U. S. Department of Commerce, Washington 25, D. C. for sale to the general public.
Stock available at OTS \$ 1.25.....

.....

Copies of ARL Technical Documentary Reports should not be returned to Aerospace Research Laboratories unless return is required by security considerations, contractual obligations or notices on a specific document.

ARL 64-27

RESEARCH ON HYPERSONIC FLOW

H. F. WALDRON
C. E. WITTLIFF
M. R. WILSON

CORNELL AERONAUTICAL LABORATORY, INC.
BUFFALO, NEW YORK

FEBRUARY 1964

Contract AF 33(616)-7812
Project 7064

AEROSPACE RESEARCH LABORATORIES
OFFICE OF AEROSPACE RESEARCH
UNITED STATES AIR FORCE
WRIGHT-PATTERSON AIR FORCE BASE, OHIO

FOREWORD

This third and final report was prepared by the Aerodynamic Research Department of Cornell Aeronautical Laboratory, Buffalo, New York, on Contract AF 33(616)-7812 for the Aerospace Research Laboratories, Office of Aerospace Research, United States Air Force. The research reported herein was accomplished on Project 7064, "Aerothermodynamic Investigations in High Speed Flow" under the technical cognizance of Col. Andrew Boreske, Jr., of the Hypersonic Research Laboratory of ARL.

ABSTRACT

This report summarizes research conducted under Contract 33(616)-7812 during the period 15 December 1960 to 15 December 1963. The theoretical and experimental investigations have been concerned with three aspects of hypersonic flow; namely, rarefied hypersonic flow about blunt axisymmetric bodies, about cylinders normal to and inclined to the free stream, and higher Reynolds number flows about pointed cones. Except for the experimental data obtained for high Reynolds number flows about pointed cones, all the research discussed in this summary report has been previously published or is in the process of publication.

TABLE OF CONTENTS

Section	Page
1.0 INTRODUCTION	1
2.0 RAREFIED HYPERSONIC FLOW ABOUT BLUNT AXISYMMETRIC BODIES	1
2.1 General Comments	1
2.2 Bow Shock and Flow Structure	3
2.3 Higher Order Rarefaction Effects	5
2.4 Experimental Investigations	5
3.0 HYPERSONIC FLOW ABOUT CYLINDERS	6
3.1 The Thin Shock Layer Theory of Flow Over Yawed Cylinders at Low Reynolds Numbers	6
3.2 An Extended Vorticity Interaction Theory	7
3.3 Experimental Investigations	8
4.0 HYPERSONIC FLOW OVER POINTED CONES	8
4.1 Theoretical Analysis of Flow Over a Yawed Cone	8
4.2 Experimental Investigations	10
5.0 CONCLUDING REMARKS	12
REFERENCES	13

OF ILLUSTRATIONS

Figure		Page
1	Rarefied Gas-Flow Regimes of a Highly Cooled Blunt Body at Hypersonic Speed	16
2	Comparison of Solutions Based on the Two-Layer Model of Levinsky and Yoshihara for the Stagnation Region at $Re_b = 25$	17
3	Shock Transition Zone and Streamline Pattern Around A Body of Hyperboloidal Shape for Successive Degrees of Rarefaction ($K^* = 1, 3, \text{ and } 10$)	18
4	Effect of Slip and Temperature Jump on Stagnation-Point Heat-Transfer Rate at High and Low Reynolds Numbers	19
5	Hemisphere-Cylinder Heat Transfer Models	20
6	Comparison of Theory and Experiment for Axisymmetric Stagnation-Point Heat Transfer at Low Reynolds Numbers	21
7	Comparison of Stagnation-Point Heat-Transfer Measurements on Spherical Bodies with Theories	22
8	Heat Transfer Distribution Around An Axisymmetric Body (Hemisphere-Cylinder)	23
9	Stagnation Streamline Heat-Transfer and Skin-Friction Characteristics of a Swept Leading Edge at Various Degrees of Sweep and Gas Rarefaction	24
10	Rate of Increase of the Chordwise Surface Stress at the Leading Edge at Various Degrees of Sweep and Gas Rarefaction	25
11	Comparison of Theory and Experiment for Stagnation Line Heat Transfer to Transverse Cylinders at Zero Yaw	26
12	Circumferential Heat Transfer on Cylinder at Zero Yaw	27
13	Comparison of Theory and Experiment for Stagnation Line Heat Transfer to Yawed Cylinders at Low Reynolds Number	28
14	Location of Heat Transfer Gauges and Pressure Transducers on the 40° Cone Model	29
15	40° Conical Body	30
16	Comparison of Pressure Rise on a 20° Half Angle Cone at Zero Yaw with a Boundary Layer Displacement Theory	31

17	Comparison of Heat Transfer (C_H) with Local Reynolds Number for a 20° Half Angle Cone at Zero Yaw with Theory	32
18	Comparison of Circumferential Pressure Distribution (Relative to Stagnation Line) (p/p_o) for a 20° Half Angle Cone at 10° Yaw with Theoretical Predictions	33
19	Comparison of Circumferential Heat Transfer Distribution (Relative to Stagnation Line) (q/q_o) for a 20° Half Angle Cone at 10° Yaw with Theoretical Predictions	34

LIST OF SYMBOLS

a	nose radius
c	constant in viscosity - temperature relation
C_H	Stanton Number
C_{fy}	coefficient of spanwise stress
C_{fx}	coefficient of chordwise stress
H	total enthalpy
H_{aw}	local adiabatic wall enthalpy
k_1	defined by $\mu = k_1 \lambda \rho \sqrt{\gamma RT}$
K^2	rarefaction parameter $\equiv \epsilon \frac{\rho_\infty U_\infty a}{\mu_0} \left(\frac{T^*}{T_0} \frac{\mu_0}{\mu^*} \right)$
K_λ^2	$\equiv \epsilon \frac{\rho_\infty U_\infty a}{\mu_0}$ w.c. Δ
M	Mach number
p	pressure
Pr	Prandtl number
P_R	shock tunnel reservoir pressure
$q, q_{B.L.}$	rate of energy transported to body surface (per unit time per unit area) and the rate of heat transfer according to boundary layer theory respectively
r	distance from axis of symmetry
Re_b	$\equiv \frac{\rho_\infty u_\infty a}{\mu_0}$
Re_f	$\equiv \frac{1}{\gamma^2} \frac{K^2}{\epsilon^2} \frac{T_0}{T^*} \frac{\mu^*}{\mu_0} \equiv \frac{Re_b}{\gamma^2 \epsilon}$
Re_x	Reynolds number $\equiv \frac{\rho u x}{\mu_0}$
R_s	radius of curvature of shock layer outer edge
T	temperature

u, v	velocity in x and y direction respectively
x, y	curvilinear coordinates; x is the distance along the surface and y is the distance normal to the surface
Y	shock layer thickness
α	angle of attack
β	shock angle
γ	ratio of specific heat
ϵ	$\equiv \frac{\gamma-1}{\gamma+1}$
ε	$\equiv \frac{\gamma-1}{2\gamma}$
Θ	half cone angle
κ	thermal conductivity
λ	mean free path
λ_s, λ_j	proportionality constants in expression for slip and temperature jump respectively (i.e. $\Delta u \equiv \lambda_s \frac{\partial u}{\partial y}$, $\Delta T \equiv \lambda_j \frac{\partial T}{\partial y}$)
Λ	yaw angle for cylindrical bodies
μ	viscosity
ρ	density
φ	circumferential angle (for yawed cones)
$\bar{\xi}$	viscous interaction parameter
Ω, Ω^*	vorticity interaction parameter as defined by Hayes and Probstein ⁷ and the vorticity interaction parameter as defined in Ref. 9 respectively
Subscripts	
∞, s, w	pertaining to free stream conditions to conditions behind the shock and to the conditions at the wall respectively
0	pertaining to stagnation conditions
i, c	flow properties with and without boundary layer interaction effects respectively

Superscripts

()*

properties are related to a reference temperature

$$T^* \left(\frac{\mu}{\mu^*} = C^* \frac{T}{T^*} \right)$$

For a blunt axisymmetric body $T^* \approx \frac{T_e + T_w}{2}$

1. INTRODUCTION

A combined experimental and theoretical investigation of the aerodynamic and thermodynamic characteristics of hypersonic flight was undertaken by Cornell Aeronautical Laboratory, Inc., under Contract No. AF 33(616)-7812. The objective of this program is to advance the understanding of hypersonic airflows particularly with respect to boundary layer behavior, to heat transfer and pressure distributions about bodies, and to rarefied-gasdynamics effects. This report summarizes the investigations conducted over the three-year period 15 December 1960 to 15 December 1963. The research is of a continuing nature having been initiated under Contract No. AF 33(616)-2387 and later supported under Contract No. AF 33(616)-6025.

During the present contract, the CAL 11 x 15-inch hypersonic shock tunnel was replaced by a new six-foot diameter tunnel. As a result of the very high expansion ratio of this facility, experimental data were obtained under this contract for hypersonic rarefied flow about bodies. The shock tunnel as operated at CAL has been established as a facility capable of hypersonic flow research at low Reynolds numbers.¹

The research conducted under this contract has been divided into three areas: namely, rarefied hypersonic flow about blunt axisymmetric bodies, about cylinders normal to and inclined to the free stream, and higher Reynolds number flows about pointed cones. The research reviewed in this summary report has been previously published or is in the process of publication except for the experimental data obtained for high Reynolds number flows about pointed cones.

As in the past, the research investigation is relied heavily on knowledge of hypersonic flow phenomena obtained not only under previous ARL contracts but also under other contracts held by the Aerodynamic Research Department of CAL. In some cases the research investigation was only partially supported by the present contract. For instance in the theoretical studies, the basic concept of the thin shock layer was developed under the Office of Naval Research Contract No. Nonr 2653(00). However, some of the subsequent applications to the blunt axisymmetric body, the cylinder, and the yawed cone were performed under the present contract. The theoretical study of the yawed cone is briefly reviewed in this report, even though the work was primarily performed under the previous contract (AF 33(616)-6025), since it has a direct bearing on the experimental program and was published in the literature in the present contractual period.

2. RAREFIED HYPERSONIC FLOW ABOUT BLUNT AXISYMMETRIC BODIES

2.1 GENERAL COMMENTS

A large body of the current literature concerns hypersonic flow at high Reynolds numbers, both viscous and inviscid, about blunt bodies. However, the corresponding problem at low Reynolds numbers has been treated much less extensively. A major portion of the investigations conducted under the present contract studied the departures of viscous flow from the classical continuum boundary layer concept due to increased flow rarefaction. The theoretical studies of these departures have utilized the Navier-Stokes equations with appropriate boundary conditions to account for surface slip effects and for the influence of transport properties throughout the entire flow field. Such approaches to the problems of rarefied gasdynamics have proved more tractable than those based on kinetic theory. A continuum flow model based on the Navier-Stokes

Manuscript released by the authors January 1964 for publication as an ARL Technical Documentary Report

equations promises a range of applicability far more extensive than previously considered.²⁻⁴ Under this contract, a solution based on continuum concepts has been developed for the entire flow field about a blunt nonslender body without the usual shock discontinuity.

Prior to reviewing the specific theoretical and experimental research, it is appropriate to describe in more detail the theoretical flow model and the assumptions. The flow field about a blunt nonslender body is assumed to be composed of two layers, an inner layer and an outer shock transition zone. It is further assumed that the shock layer is thin in comparison with the body, and that the shock is strong. The latter two assumptions imply a high shock compression ratio.

For the stagnation region in hypersonic flow about a blunt body, Probstein and Kemp³ have defined six flow regimes between the classical boundary layer and the free molecule flow regimes. These regimes are illustrated in Fig. 1 as a function of altitude and velocity for a vehicle with nose radius of one foot. Based on the concept of a thin shock layer, Cheng^{5,6} has shown that only two regimes need be defined for a consistent treatment of the flow up to and including part of the fully merged layer regime of Probstein and Kemp. These regimes are based on two parameters ϵ and K^2 such that

$$\text{in Regime I} \quad O(1) \leq \epsilon K^2 < \infty$$

$$\text{and Regime II} \quad O(\epsilon) \leq \epsilon K^2 \leq O(1)$$

the parameters ϵ and K^2 are given by

$$\epsilon \equiv \frac{\gamma-1}{2\gamma}$$

and

$$K^2 \equiv \epsilon \frac{\rho_\infty U_\infty a}{\mu_0} \left(\frac{T^* \mu_0}{T_0 \mu^*} \right)$$

where γ is the ratio of specific heats

ρ_∞, U_∞ are the free-stream density and velocity respectively

T, μ are temperature and viscosity of the gas respectively, the subscript 0 refers to stagnation conditions and * refers to a reference temperature (to be discussed later)

a is the nose radius

The two flow regimes are shown in Fig. 1 where it is seen that Regime II includes a major portion of the fully merged layer regime of Probstein and Kemp where the shock layer and the shock transition zone are comparable in thickness. The parameter K^2 is a measure of the over-all transport processes and is essentially a local Reynolds number. It can also be related to the Knudsen number λ_∞/a as $K^2 \sim \sqrt{\epsilon} a/\lambda_\infty$. At the lower Reynolds number, in Regime II, the normal Rankine-Hugoniot relations are modified due to transport behind the shock; whereas, at the higher Reynolds number, in Regime I, the usual Rankine-Hugoniot shock relations are valid.

In the analysis of flow field based on the thin shock layer concept, a linear viscosity-temperature relation is assumed of the form

$$\mu = \mu^* \frac{T}{T^*}$$

and the reference temperature T^* is chosen as

$$T^* = \frac{T_s + T_w}{2} \approx \frac{T_o + T_w}{2}$$

where T_s and T_w are temperatures immediately behind the shock and at the body surface respectively. However, the assumption of a linear viscosity-temperature relation may lead to solutions far different from the solution using the more exact viscosity-temperature relation.⁷ This discrepancy has been studied under the present contract and it has been shown⁸ that, provided an appropriate reference temperature is chosen, a linear viscosity-temperature relation is adequate for most purposes in high and low Reynolds number flows. A relation of the form $\mu \sim T^\omega$ was selected. For $\omega = 0.65$ the viscosity for air agrees reasonably well with that obtained from the Sutherland law in the range of $T = 500^\circ$ to 3000° K. Based on this value of ω , the values of skin friction, heat transfer, enthalpy behind the shock, and the shock stand-off distance have been computed and compared with the value obtained from the linear viscosity-temperature relation for a Prandtl number $Pr = 0.71$, $\epsilon = 0.10$ and $T_w/T_o \rightarrow 0$. In the two flow regimes obtained from the thin shock layer analysis, the difference in the above quantities calculated from the two viscosity laws is at most 4%.⁸

Also under this contract an extended vorticity-interaction theory has been developed for an axisymmetric blunt body using the thin shock layer concept. Numerical solutions have been obtained⁹ over an extensive range of the vorticity-interaction parameter for $Pr = 0.71$, and $T_w/T_o = 0.40$ and $T_w/T_o \rightarrow 0$. The vorticity-interaction parameter used in these calculations (Ω^*) differs from that used by Hayes and Probst⁷ (Ω) in calculating the value of heat transfer. The relation between the two vorticity-interaction parameters is given by

$$\frac{\Omega}{\Omega^*} = \sqrt{\frac{\mu_o}{\mu^*} \frac{T^*}{T_w}}$$

Calculations based on Ω give rise to infinite heat transfer rates as $T_w/T_o \rightarrow 0$ since $\Omega \rightarrow \infty$. However, the use of the parameter Ω^* which does not critically depend on surface temperature yields finite values of heat transfer rate as $T_w/T_o \rightarrow 0$.

2.2 BOW SHOCK AND FLOW STRUCTURE

Under the present contract, the thin shock layer concept has been applied to the analysis of the structure of the bow shock produced by a blunt axisymmetric body in a rarefied hypersonic flow.¹⁰ Also, the consistency of the solution based on the two-layer formulation (i.e. the shock transition zone and the shock layer) with the solution to the Navier-Stokes equations based on an asymptotic expansion procedure has been examined.¹⁰ These analyses are complementary to and an amplification of a previous development⁶ sponsored by the Office of Naval Research Contract No. 2653(00). In the previous development numerical solutions for the shock layer were presented. With modified Rankine-Hugonot relations the flow field in the shock layer can be determined independent of the flow in the shock

transition zone.

Underlying the two-layer concept is the idea of two matched solutions each representing an asymptotic development for small ϵ and $Re_b \equiv \frac{\rho_0 u_0 a}{\mu_0}$. Recently, by considering four separate flow regions, Bush¹¹ has formulated the problem strictly through the use of asymptotic expansions. In Ref. 10, the asymptotic expansion procedure is compared with that based on the two-layer model for small ϵ , $1/Re_b$ and $1/\epsilon M_\infty^*$. The solutions based on the two formulations are found to be consistent to the first approximation throughout the entire flow field. The two-layer model provides a uniformly valid approximation to the Navier-Stokes equations for the tangential velocity, total enthalpy, and temperature as well as the streamline pattern around simple blunt bodies. This does not hold for the solution of the normal velocity near the downstream end of the shock transition zone, since the variation in normal velocity in this region is too small to be evaluated by a first-order theory. In either formulation of the problem, it is necessary to match solutions of the two neighboring principal regions over a region intermediate between the two regimes under consideration. However, it is not possible in either formulation to match exactly solutions in the two regions. A smooth composite solution describing the whole field has not as yet been demonstrated.

In the analysis of the shock transition zone, the interaction of the nonuniform downstream flow with the shock transition zone is included. This interaction appears primarily in the adjustment of the shock structure to the highly nonuniform downstream velocity and temperature fields. In the previous analysis,⁶ a numerical solution for the flow field has been compared with a more exact numerical solution for the stagnation region of a sphere by Levinsky and Yoshihara.¹² In the present work, an analytical solution for the shock transition zone has been obtained for the case of a plane shock; this solution is compared with the solution due to Levinsky and Yoshihara in Fig. 2. It is seen that the two solutions agree in all essential details.

The current work has also included the calculation of the streamline pattern, the temperature field and the shock thickness around a highly cooled axisymmetric body of hyperboloidal shape at low Reynolds number. These calculations are based on the analytical solution of the shock transition zone (discussed above) and the previous numerical solution of the shock layer.⁶ The results for the streamline pattern for three values of the rarefaction parameter ($K^* = 1, 3, 10$) are given in Fig. 3. At $K^* = 3$, it is noted that the shock layer and the shock transition zone over the forward portion of the body are already comparable in thickness. The streamlines are bent only slightly in the shock transition zone. The corresponding temperature profiles given in Ref. 10 show that the temperature is everywhere lower than that obtained from inviscid theory. The maximum temperature, obtained in the transition zone, is 0.86 of the free stream stagnation temperature. The flow fields obtained from these calculations for infinite Mach number are characterized by a sharp frontal surface which separates the disturbed flow region from the upstream uniform flow.

The current work described in detail in Ref. 10 has provided an analytical solution of the shock structure which is compatible with the previous shock layer solution⁶ and which takes into account the non-uniformity of the downstream flow. This solution provides for the first time a description of the temperature profiles

and streamline patterns of a hypersonic flow field about a body without the usual shock discontinuity.

2.3 HIGHER-ORDER RAREFACTION EFFECTS

In the study of the bow shock structure and shock layer discussed above, second order effects associated with terms of order ϵ and $1/Re_b$ were neglected. However, Ref. 10 also examines the consequences of two higher order effects; namely, finite shock thickness, and velocity slip and temperature jump at the body surface.

The shock thickness effects associated with losses of mass, momentum, and energy fluxes to the transition zone have been analyzed. It is shown¹⁰ that while effects resulting from each of these losses is generally of order $\ln \epsilon / Re_b$, that their combined effect on heat transfer, skin friction and most properties of the shock layer is weaker being of order of Re_b^{-1} . Thus, the order of magnitude of the shock-thickness effect in the downstream flow becomes no larger than the longitudinal and transverse curvature effects.

The current investigation has also provided an analysis of the slip and temperature jump effects at the stagnation region for an axisymmetric body in the range of $K^2 \approx O(1)$. The solution obtained provides an explicit, analytical formula for stagnation point heat transfer incorporating slip and temperature jump in terms of the no-slip, stagnation-point heat transfer. This formula correlates the results of Rott and Lenard¹⁵ obtained for high Reynolds numbers and thus may serve as a universal formula for the slip correction at all Reynolds numbers. The effect on heat transfer is shown in Fig. 4 where the solid curve represents the solution without slip, but includes the effects of transport behind the shock (i. e. based on modified Rankine-Hugoniot relations). The lower broken curve represents the value of heat transfer obtained from the analytical formula including correction for slip effects at the body surface. The upper broken curve is calculated from a nonlinear vorticity-interaction theory (corresponding to the viscous layer⁶) which uses the unmodified Rankine-Hugoniot shock conditions. The departure of this curve from the solid curve represents the magnitude of the transport effects behind the shock or the magnitude of the "slip effects" at the outer edge of the shock layer. From Fig. 4 it is evident that the surface slip and temperature jump effects on a cooled surface are relatively insignificant compared to the slip-like (transport) effects at the outer edge of the shock layer.

The analysis given in Ref. 10 of the shock thickness and surface slip effects has established that the error in the shock layer solution based on the present formulation is no larger than $1/Re_b^2$, $1/Re_b$ and $\sqrt{\epsilon} \frac{T_w}{T_0} C_H$.

2.4 EXPERIMENTAL INVESTIGATIONS

The first low density experiments at CAL using a blunt axisymmetric model were performed under the Office of Naval Research Contract No. Nonr 2653(00).^{15, 16} The current experimental results (reported in Ref. 17) conducted in the CAL 1.5-foot shock tunnel have extended those results to an order of magnitude lower in Reynolds number. The hemisphere cylinder models used in this program varied in diameter from 1/8" to 2" and are shown in Fig. 5. Only the largest model (2" diameter) was equipped with heat transfer gauges away from the stagnation point.

In Fig. 6, the data obtained from the previous and the present contract are compared with Cheng's⁵ viscous shock layer theory. The various low density regimes as proposed by Probst and Kemp³ can be easily correlated to the value of K^2 by computing the Knudsen number λ_∞/a . At the lowest value of K^2 (about 0.1) the free stream Knudsen number is of the order of unity. This represents approximately the boundary between the fully merged layer and the transitional regimes. At a higher value of K^2 (about 10), the corresponding free stream Knudsen number is about 5×10^{-3} which is in the vorticity interaction regime near the boundary of the viscous layer regime. It is seen that Cheng's⁵ theory which is based on only two regimes correlates well with the experimental data, in spite of the fact that the validity of the theory is only of order ϵ , corresponding to about 0.085 for K^2 of the order of unity.

The experimental data for heat transfer are compared in Fig. 7 with other experimental data and other theories as $q/q_{s.p.}$ vs Re_f , where q is the stagnation point heat transfer rate measured on a small sphere and $q_{s.p.}$ is the heat transfer rate corresponding to vanishing vorticity. The Reynolds number Re_f is related to K^2 as

$$Re_f \approx \frac{1}{\sqrt{2}} \left(\frac{T_0}{T^*} \frac{\mu^*}{\mu_0} \right) \frac{K^2}{\epsilon^2}$$

In the higher Reynolds number range ($Re_f \geq 500$) there is a rise over the boundary layer value due to the external vorticity effect. In the lower Reynolds number range ($Re_f \leq 500$) the heat transfer ratio begins to decrease and goes below unity approaching the free molecule limit. Towards the higher Reynolds number end the data of Ferri et al¹⁸ agree well with their own predictions but appear to be higher than the thin-shock-layer analysis. The current CAL data give reasonable agreement in view of the scatter of data and the accuracy of the thin-shock-layer analysis at the very low Reynolds numbers.

In Fig. 8 heat transfer data are presented for flow around a hemisphere cylinder body at points removed from the stagnation region.¹⁷ It is seen that there is no change in heat transfer distribution for the range of free stream Knudsen number from 10^{-2} to 10^{-1} . The theoretical distribution obtained by Lees¹⁹ for a laminar boundary layer is also given in Fig. 8. Except in the vicinity of 45° and 90° , the agreement is good. The data are plotted as the ratio of heat transfer to the heat transfer at the stagnation point.

3. HYPERSONIC FLOW ABOUT CYLINDERS

3.1 THIN SHOCK LAYER THEORY OF FLOW OVER YAWED CYLINDERS AT LOW REYNOLDS NUMBER

The thin shock layer concept has been discussed under Section 2.1. Under the present contract this two layer formulation has been adapted to the low Reynolds number flow over a yawed cylinder.⁹ The solution of the resultant equations provides the local distribution of velocity parallel to the surface, the spanwise velocity and the enthalpy as a function of the rarefaction parameter for yawed bodies

$$K_\Lambda^2 = \frac{\epsilon \rho_\infty U_\infty a}{\mu_0} \sin \Lambda$$

where Λ is angle of yaw. Numerical solutions have been obtained in the region close to the stagnation streamline under the assumption of a unit Prandtl number, a viscosity-temperature relation of the form $\mu \sim T^{1/2}$, $\epsilon = 1/8$, and a surface-to-stagnation temperature of 1/7. The calculations cover a range of yaw angles from 0° to 60° and a range of rarefaction $0.3 \leq K^2 \leq 20$. In this regime departures from the boundary layer limit are appreciable, but the shock layer concept is applicable.

The coefficients of heat transfer (C_H), of spanwise stress (C_{f_s}) and of chordwise stress (C_{f_x}) as computed in Ref. 9 are given in Figs. 9 and 10. The surface heat transfer and surface stresses generally approach the classical boundary layer value from above and the free molecule limit from below, except the chordwise stress coefficient (C_{f_x}) which overshoots the free molecule limit at a finite K_A^2 at the larger yaw angles. The increase in spanwise stress and heat transfer rate above the boundary layer predictions at intermediate values of K_A^2 is considerably less than for the axisymmetric case. This is due to the fact that vorticity interaction is a higher order effect for flow about cylinders.

The surface heat transfer and enthalpy profile are shown to be relatively insensitive to yaw at small and moderate values of yaw. This suggests that for heat transfer a yaw independence principle may be valid. A study of the governing equations indicates that the accuracy of such a principle is controlled by the Prandtl Number, the viscosity-temperature relation and the surface to stagnation temperature ratio. The influence of the spanwise velocity on the profiles of chordwise velocity and enthalpy appear mainly through the change of the local density ratio ρ_w/ρ . This ratio in turn controls the chordwise pressure gradient effect (i. e. $\partial/\partial x$). For a comparatively cold surface, $T_w/T_0 \leq 1$ the density ratio changes only slightly except at large yaw angles. The rules of correlation for this independence principle are developed in Ref. 9 and are consistent with results previously obtained by Reshotko and Beckwith¹⁴ for the compressible laminar boundary layer. The yaw independence principle does not imply a complete independence of spanwise velocity; however, it does provide a means for correlating heat transfer on a yawed cylinder with the heat transfer on a cylinder at a different yaw and at a different Reynolds number.

3.2 AN EXTENDED VORTICITY INTERACTION THEORY

In the higher Reynolds number regime $K^2 \geq O(1)$ the transport effect behind the shock is small and the ordinary Rankine-Hugoniot relations are applicable. Since the external vorticity is inversely proportional to shock layer thickness, its influence on the viscous layer is large for the thin shock layer considered. As a result of the thin shock layer assumptions the equations governing the shock layer are reducible to a form equivalent to those in the vorticity interaction theory (for the axisymmetric case) of Hayes and Probstein (these were derived from the boundary layer equations in the weak interaction field).

In the present study, numerical solutions have been obtained and presented⁹ for both axisymmetric and plane flow cases. These calculations cover an extensive range of vorticity interaction parameters for $\Pr = .71$ and a cold surface $T_w/T_0 \rightarrow 0$.

The major advantage of this treatment of the vorticity interaction regime is that the specific heat and Reynolds number are combined into one parameter and

that the flow field can be solved without the determination of shock position. In the earlier work of Hayes and Probstein⁷ a different vorticity interaction parameter (Ω) is used. There as $T_w/T_o \rightarrow 0$, $\Omega \rightarrow \infty$ thus for the theory breaks down. However, in the present CAL analysis the vorticity interaction parameter Ω^* remains finite and thus the solution is valid as $T_w/T_o \rightarrow 0$. In this analysis the solution is not restricted to the range of small Ω^* as in the case in the Hayes and Probstein theory.

3.3 EXPERIMENTAL INVESTIGATIONS

A series of experiments were conducted under this contract in which heat transfer was measured to circular cylinders at 0°, 15°, 30° and 45° yaw. The cylinder models varied in size from 1/8 to 2 1/8 inches. The 1/8 and 1/2 inch models each had a single heat transfer gauge on the forward stagnation line. To check end effects the 1/4 and 2 1/8 inch models each had three heat transfer gauges longitudinally spaced about one inch apart along the forward stagnation line. The one-inch circular cylinder was instrumented with thirteen gauges spaced at 15° intervals around the circumference at one longitudinal position.

This experimental investigation has been reported in more detail in Ref. 17. Typical experimental data for zero yaw are presented in Fig. 11 as the Stanton number vs. the rarefaction parameter K^* and compared both with Cheng's viscous shock layer theory⁹ and with Cohen and Reshotko's compressible boundary layer theory.²⁰ In Fig. 12 the ratio of circumferential heat transfer to that at the stagnation point for a transverse cylinder at zero yaw is presented. The data are plotted on a logarithmic scale to show the influence of Reynolds and Knudsen number on the distribution in the separated flow region. Also shown is the empirical relation obtained by Tewfik and Giedt²¹ based on their low Mach number data. The laminar boundary layer of Beckwith²² is also shown in Fig. 12. Better agreement is obtained with the theoretical curve than with the empirical relation obtained at low Mach number.

In Fig. 13 the experimental data expressed in terms of $C_H / \cos \alpha$ are presented as a function of the rarefaction parameter for yawed cylinders and compared with the viscous layer theory of the yawed cylinder reviewed in Section 3.1. Since the scatter in the data is greater than the difference between the two theoretical curves for zero and 45° yaw, a confirmation of the yaw independence principle is not possible. However, no separation in the 0° and 45° data is discernible.

4. HYPERSONIC FLOW OVER POINTED CONES

4.1 THEORETICAL ANALYSIS OF THE INVISCID FLOW ABOUT A YAWED CONE AND OTHER POINTED BODIES

The original theoretical analysis of inviscid hypersonic flow about yawed cones and other pointed bodies was performed and reported in Ref. 23 under an earlier ARL sponsored program (AF 33(616)-6025). A paper on this analysis was published in the Journal of Fluid Mechanics²⁴ under the current contract. The analysis, viewed briefly in this section, provides a detailed treatment within the framework of shock layer theory of the inviscid hypersonic flow past a circular cone at small and moderate yaw angles. Also given in Ref. 24 is an analysis of the three dimensional flow field with special reference to the flow structure near the surface of a pointed, but otherwise arbitrary body.

In the analysis of the flow about a yawed cone, a singularity occurs at its surface. Ferri²⁵ first hypothesized the existence of a region of intense vorticity next to the body (i. e. a vortical layer). The presence of such a layer implies that analyses of the cone problem in which the layer is neglected yield incorrect values of the entropy on the cone surface. Cheng,^{23, 24} utilizing the shock layer theory and small perturbations in the yaw angle, has obtained a uniformly valid solution for the flow over a yawed cone. The solution provides explicit relations for the flow at the inner edge of the shock layer including the effect of the vortical layer. A valid first order approximation to the entropy field is obtained except in the neighborhood of the stagnation streamline on the lee side of the cone. Relations for first order approximations of the density, pressure, radial velocity and circumferential velocity have been obtained.* Formulas valid to the second order have been obtained for the pressure and the circumferential velocity fields. These results show that the streamline at the inner edge of the shock layer must closely follow the generator of the cone surface in a manner independent of the yaw angle.

The development of the entropy relation,²⁴ including the singularity at the cone surface, provides a relation for the radial velocity about a yawed cone which includes the effect of the vortical layer. It is shown that in supersonic flow the existence of the vortical layer is dependent on a small yaw angle; in hypersonic flow a thin vortical layer can exist even if the yaw angle is not small. The angular thickness of the vortical layer is considerably less than anticipated by Ferri,²⁵ being much less than $\alpha \epsilon^{\frac{1}{2}}$ where α is the angle of attack and $\epsilon = \gamma - 1 / \gamma + 1$ (γ is the ratio of specific heats). It is also shown²⁴ that the effect of the vortical layer on circumferential velocity and pressure belongs at most to the second order in ϵ and angle of attack.

The study has also been extended²⁴ to a more general case in which the specific assumptions of small yaw angle and of circular cone are not required. This study indicates that flow speed and enthalpy persist along the streamline and that fluid particles tend to travel the shortest path on the body surface (i. e. along the surface geodesic). At the surface of a pointed body the inviscid streamline geodesics approach the pattern of the family of geodesics originating from the pointed nose irrespective of the angle of attack. A thin vortical layer generally appears at the inner edge of the shock layer around a three dimensional pointed body. At the base of the vortical layer the entropy, flow speed and enthalpy are essentially uniform.

The existence of the thin vortical layer indicates the importance of outer-flow vorticity to the boundary layer development over a pointed three dimensional body. In the supersonic case the existence of the vortical layer is not too important. In the hypersonic case, where large variations in the outer entropy field are present, the vortical layer assumes much greater importance. The present analysis (given in detail in Refs. 23 and 24) has shown the thickness of the vortical layer to be small. Thus its effect may not be too significant when the boundary layer has an appreciable thickness, even in the hypersonic case.

* In a recent publication²⁶ an algebraic error in the calculation of entropy has been noted. The corrected values for both the first and second order approximations for the flow field are given in Ref. 26.

4.2 EXPERIMENTAL INVESTIGATIONS

A previous investigation of hypersonic flow about cones was performed and reported under an earlier ARL contract (AF 33(616)-6025) and was recently published.²⁷ The investigation of hypersonic flow about cones was extended under the present contract to the measurement of heat transfer and pressure distribution on a 20° half angle cone at zero yaw and 10° yaw. The cone angle and angle of attack were chosen to conform with the assumptions of Cheng's theoretical analysis so that the validity of his theoretical analysis might be experimentally investigated. This experimental investigation was performed in the CAL six-foot hypersonic shock tunnel at free stream Mach numbers 19 to 25 and at free stream Reynolds numbers $3.3 \times 10^3 \text{ ft}^{-1}$ to $7.9 \times 10^4 \text{ ft}^{-1}$. The cone model was equipped with heat transfer gauges and pressure transducers to permit circumferential and axial measurements. A schematic diagram of the cone showing gauge location is given in Fig. 14. A photograph of the model with a conical afterbody is shown in Fig. 15.

At relatively small angles of attack flow angularity in the shock tunnel may affect data measured on the cone surface. A technique to measure flow angularity to a high degree of accuracy was developed under the joint sponsorship of the present contract and contract AF 49(636)-952. A flow angularity rake consisting of two parallel flat plates equipped with heat transfer gauges was constructed with CAL funds. When the plates are aligned with the flow in the test section of the shock tunnel, the two plates experienced equal heat transfer. These tests revealed a downflow in the tunnel of about 0.15° and a cross flow of about 0.2°. For the current investigation of heat transfer and pressure distribution about a large angle cone, the influence of this small flow angularity in the test section was negligible.

Typical pressure data for the 40° angle cone at zero yaw are given in Fig. 16. The pressure data are given as the ratio of measured cone pressure to the pressure predicted by conical flow theory $(p_c/p_c - 1)$ as a function of the viscous interaction parameter $(\bar{r}_c = M_c \sqrt{\frac{c}{Re_x}})$ based on local flow conditions. (M_c is the local Mach number, c the constant in the viscosity-temperature relation and Re_x the local Reynolds number.) The pressure p_c has been obtained from Kopal's tables.²⁸ The experimental data are compared with Probstein's²⁹ analysis based on the induced pressure rise due to boundary-layer displacement for a wall to stagnation-temperature ratio T_w/T_0 of 0.1. It is noted that reasonable agreement between the experimental data and Probstein's analysis is obtained, although the general trend appears to indicate a larger experimental pressure rise.

The corresponding heat-transfer data in terms of the Stanton number $[C_H = q/\rho_c u_c (H_{a,w} - H_w)]$ is given in Fig. 17 as a function of the local Reynolds number. (The Stanton number is based on the local flow velocity u_c , the local density ρ_c and the difference between the local adiabatic-wall enthalpy and the enthalpy at the wall temperature.) The experimental results are compared with Probstein's analysis²⁹ in which the effect of boundary-layer displacement and transverse curvature are included and with the laminar boundary layer theory, given by

$$C_H = 0.3321 \sqrt{3} Pr^{-2/3} \sqrt{\left(\frac{c}{Re_x}\right)}$$

Probstein has shown theoretically that transverse curvature may have a significant effect on the heat transfer whereas the boundary-layer displacement has a much

smaller effect. In the present experimental study with a 40° total angle cone no significant transverse-curvature effect is present. It is seen that no significant departure of the heat transfer from laminar-boundary theory is observed even though the pressure data indicate a large boundary-layer-displacement effect.

In Figs. 16 and 17 separate symbols are used for the experimental data obtained at various shock-tunnel-reservoir pressures (P_R). For the two lower reservoir pressures ($P_R = 500$ and 1600 psi) the experimental data have been corrected for nonequilibrium nozzle expansion in the manner described in Ref. 17.

For an angle of yaw of 10°, the circumferential-pressure distribution is given in Fig. 18 as the ratio of the pressure at angular position φ to the pressure at the stagnation line. The theoretical pressure distribution as given by the first and second order approximations of Ref. 24 and as given by simple Newtonian theory, (i. e. pressure coefficient $C_p = 2 [\cos \alpha \sin \theta - \sin \alpha \cos \theta \cos(180 - \varphi)]^2$ where α is angle of attack θ is cone half angle and φ the circumferential angle $\varphi = 0^\circ$ at the forward stagnation line) are compared with the experimental data. The second order approximation is almost identical to the simple Newtonian theory. It is noted that the best agreement with the experimental data is obtained with the second order relation. It should also be noted that although significant boundary-layer-displacement effects were present in the zero yaw data (under similar free stream conditions), the ratio of circumferential to stagnation-line pressure agrees reasonably well with a theory in which no interaction between the viscid and inviscid flow field is considered.

In Fig. 19 the ratio of the heat transfer at the angular position φ to the heat transfer at the stagnation line is compared with the theoretical predictions.²⁴ Since in the experimental program the value of the heat transfer at the stagnation line was not measured, the measured values of heat transfer at the angular position $\varphi = 30^\circ$ were extrapolated to the stagnation line by means of the first-order relation and the heat transfer relationship based on local similarity

$$C_H = \frac{q}{\rho_\infty U_\infty (H_\infty - H_w)} = 0.332 \left(\frac{c U_1}{Re_{x_\infty} U_\infty} \right)^{1/2} \frac{\frac{P}{P_\infty} r}{\left[\int_0^r \frac{P}{P_\infty} r^2 d\left(\frac{r}{L}\right) \right]^{1/2}}$$

where U_1 is the velocity at the outer edge of the boundary layer

r is the distance of the body from the axis of symmetry ($r = r \sin \theta$)

L is the length of the cone

and the subscript ∞ refers to the free stream conditions. Using the above relationship the heat-transfer ratio reduces simply to the square root of the pressure and the external velocity ratios. In Fig. 19, the theoretical heat-transfer has been obtained by means of the first and second order approximation for the inviscid field. Also, the value of heat transfer has been calculated using the correction for the external velocity field as given in Ref. 24 due to the presence of a vortical layer

$$\frac{U}{U_\infty} = \cos \theta - \frac{\epsilon}{2} (1 + K) \sin \theta \tan \theta$$

where θ is the cone half angle, $\epsilon = \frac{\gamma - 1}{\gamma + 1}$ and

$$K \text{ is } \frac{1}{\gamma \epsilon M_\infty^2 \sin^2 \alpha}$$

Since the velocity is now independent of angular position, the heat-transfer ratio reduces simply to the square root of the pressure ratio. The pressure ratio is unaffected by the vortical layer to the third order of $(\epsilon + \sigma)$,

$$\left(\sigma = \frac{\sin \alpha}{\sin \theta}\right).$$

Although the effect of the vortical layer is to reduce the heat transfer, the experimental data is still somewhat lower than that predicted theoretically. This discrepancy has not as yet been investigated. The experimental data at $\varphi = 30^\circ$ was extrapolated to the stagnation line by means of the first order approximations to the inviscid flow. If the heat-transfer distribution predicted by the relation incorporating the effect of the vortical layer is used to extrapolate the data from $\varphi = 30^\circ$ to $\varphi = 0^\circ$, the result is to increase slightly the discrepancy.

5. CONCLUDING REMARKS

The research investigations conducted under Contract No. AF 33(616)-7812 in the three year period ending 15 December 1963, have been briefly summarized in this report. The theoretical studies have utilized a continuum flow model based on the thin shock-layer concept. For the first time a description of the entire hypersonic flow field about a blunt non-slender body at low Reynolds numbers has been obtained without the usual shock discontinuity. A study of the velocity slip and temperature jump at the stagnation point of a blunt axisymmetric body has revealed that the slip effects are relatively minor (for heat transfer and other properties of the shock layer) compared to the "transport or "shock slip" effects behind the shock wave. Experimental measurements of heat transfer to blunt axisymmetric bodies have been extended to low Reynolds numbers under this contract and generally confirm theoretical predictions.

The thin shock layer concept was also used to compute the flow field about yawed cylinders. Experimental measurements of heat transfer generally confirm the theoretical predictions.

The inviscid flow over pointed non-slender circular cones and other pointed bodies has been analyzed within the framework of the thin shock-layer concept. Of particular importance is the calculation of the effects of a thin vortical layer (i. e. a layer of high vorticity) at the base of the shock layer. This layer has been shown to have a negligible effect on free stream surface pressure but a non-negligible effect on the inviscid radial velocity under certain flow conditions. Experimental data on the circumferential heat transfer and pressure about a non-slender cone have been obtained at hypersonic speeds and high Reynolds numbers and compared with simple Newtonian theory and Cheng's theoretical predictions. In general, the agreement is reasonable.

REFERENCES

1. Wittliff, C. E. and Wilson, M. R. Low Density Research in the Hypersonic Shock Tunnel. Rarefied Gas Dynamics. Editor, L. Talbot, Academic Press, 1961.
2. Adams, M. C. and Probst, R. F. On the Validity of Continuum Theory for Satellite and Hypersonic Jet Propulsion. Vol. 28, No. 2, p. 86, February 1958.
3. Probst, R. F. and Kemp, N. Viscous Aerodynamic Characteristics in Hypersonic Rarefied Gas Flow. Journal Aero/Space Sci., Vol. 27, No. 3, p. 174, March 1960.
4. Van Dyke, M. A Review and Extension of Higher Order Hypersonic Boundary Layer Theory. Rarefied Gas Dynamics. Editor, J. A. Laurmann, Academic Press, 1963.
5. Cheng, H. K. Hypersonic Shock Layer Theory of the Stagnation Region at Low Reynolds Numbers. Proc. Heat Transfer and Fluid Mechanics Institute. Stanford University Press, p. 161, June 1961. Also CAL Rept. No. AF-1285-A-7.
6. Cheng, H. K. The Blunt Body Problem in Hypersonic Flow at Low Reynolds Number. IAS Paper No. 63-92. Also CAL Rept. No. AF-1285-A-10.
7. Hayes, W. D. and Probst, R. F. Hypersonic Flow Theory. Academic Press, 1959.
8. Cheng, H. K. and Chang, A. L. Stagnation Region in Rarefied High Mach Number Flow. AIAA Journal, Vol. 1, No. 1, p. 231, January 1963.
9. Cheng, H. K. and Chang, A. L. Hypersonic Shock Layer at Low Reynolds Number - The Yawed Cylinder. ARL Rept. 62-453, October 1962.
10. Cheng, H. K. and Chang, A. L. On Bow-Shock and Flow Structure, Slip and Other Rarefaction Effects in Low-Density Hypersonic Flow. To be submitted for publication as an ARL report.
11. Bush, B. On the Viscous Hypersonic Blunt Body. Ph. D. Thesis, California Institute of Technology, 1963.
12. Levinsky, E. S. and Yoshihara, H. Rarefied Hypersonic Flow Over a Sphere. Hypersonic Flow Research. Editor, F. R. Riddell, Academic Press, 1962, p. 81.
13. Rott, N. and Lenard, M. The Effect of Slip Particularly for Highly Cooled Walls. Journal Aero/Space Sci., Vol. 20, No. 5, p. 591, May 1962.
14. Reshotko, E. and Beckwith, I. E. Compressible Laminar Boundary Layer Over a Yawed Infinite Cylinder with Heat Transfer and Arbitrary Prandtl Number. NACA Rept. 71379, 1958.

15. Wittliff, C. E. and Wilson, M. R. Low Density Stagnation-Point Heat Transfer in Hypersonic Air Flow. CAL Rept. No. AF-1270-A-3. ARL-TR 60-333, February 1961.
16. Wilson, M. R. and Wittliff, C. E. Low Density Stagnation Point Heat Transfer: Measurements in the Hypersonic Shock Tunnel. ARS Journal, Vol. 32, No. 2, p. 275, February 1962.
17. Vidal, R. J. and Wittliff, C. E. Hypersonic Low-Density Studies of Blunt and Slender Bodies. Rarefied Gas Dynamics. Editor, J. A. Laurmann, Academic Press, 1963.
18. Ferri, A., Zakkay, V. and Ting, L. On Blunt-Body Heat Transfer at Hypersonic Speed and Low Reynolds Numbers. Journal Aero/Space Sci., Vol. 29, No. 7, p. 882, July 1962.
19. Lees, L. Laminar Heat Transfer over Blunt-Nosed Bodies at Hypersonic Flight Speeds. Jet Propulsion, Vol. 26, No. 4, p. 259, April 1956.
20. Cohen, C. B. and Reshotko, E. Similar Solutions for the Compressible Laminar Boundary Layer with Heat Transfer and Pressure Gradient. NACA Rept. 1293, 1956.
21. Twefik, O. K. and Geidt, W. H. Heat Transfer Recovery Factor and Pressure Distributions Around a Circular Cylinder Normal to a Supersonic Air Stream. Journal Aero/Space Sci., Vol. 27, No. 10, pp. 721-729, October 1960.
22. Beckwith, I. Theoretical Investigation of Laminar Heat Transfer on Yawed Infinite Cylinders in Supersonic Flow and a Comparison with Experimental Data. NACA RML 55F09, 1955.
23. Cheng, H. K. Hypersonic Shock-Layer Theory of a Yawed Cone and Other Three Dimensional Pointed Bodies. WADC TN 59-335, 1959.
24. Cheng, H. K. Hypersonic Flow Past a Yawed Circular Cone and Other Pointed Bodies. Journal Fluid Mechanics, Vol. 12, No. 2, p. 169, February 1962.
25. Ferri, A. Supersonic Flow Around Circular Cones at Angles of Attack. NACA Rept. 1056, 1951.
26. Sapunko, I. G. Hypersonic Flow Past a Cone at Angle of Attack. PMM, Vol. 27, No. 1, pp. 190-192, 1963.
27. Wittliff, C. E. and Wilson, M. R. Heat Transfer to Slender Cones in Hypersonic Air Flow, Including Effects of Yaw and Nose Bluntness. WADD TN 59-6, December 1960. Also Journal Aero/Space Sci., Vol. 29, No. 7, July 1962.
28. Kopal, Z. Tables of Supersonic Flow Around A Cone. M. I. T. Department of Electrical Engineering Tech. Rept. No. 1, 1947.

29. Probstein, R. F. Interacting Hypersonic Laminar Boundary Layer Flow Over a Cone. Brown University, Division of Engineering Tech. Rept. AF 279811 (AD66227) March 1955.

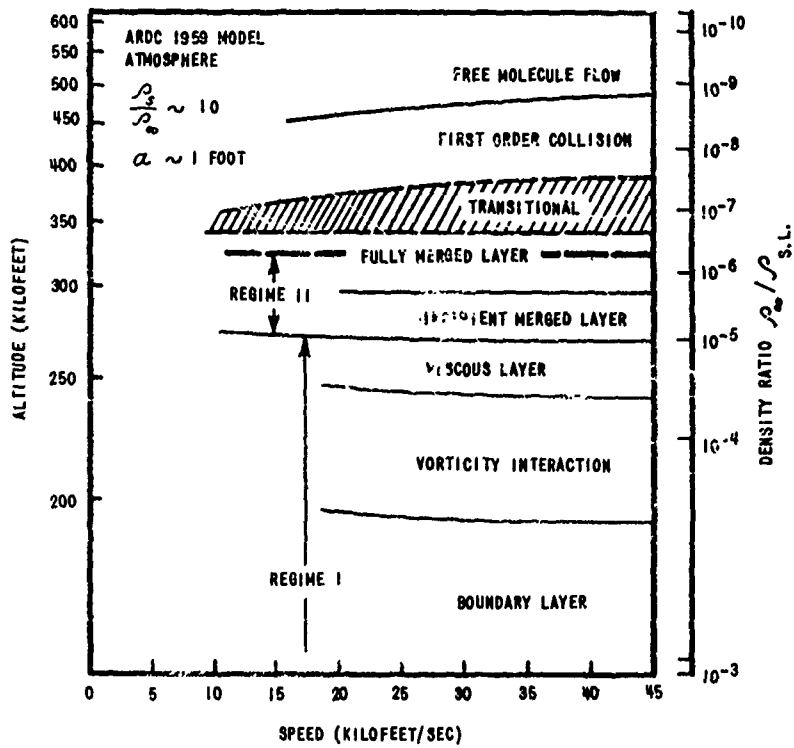


Figure 1 RAREFIED GAS-FLOW REGIMES OF A HIGHLY COOLED BLUNT BODY AT
HYPERSONIC SPEED (BOUNDARIES BASED ON DATA OF PRÖBSTEIN)

— LEVINSKY AND YOSHIHARA $\left(Re_b = \frac{\rho_\infty U_\infty a}{\mu_0} \approx 25, M_\infty = 10 \right)$
 $\left(\gamma = 5/3, T_w/T_0 = 0.0291, Pr = 0.75 \right)$

- - - PRESENT ANALYSIS $\left(K_0^2 = \epsilon Re_b = 5, \epsilon = 1/5, \right)$
 $\left(T_w/T_0 = 0.0291, Pr = 0.75 \right)$

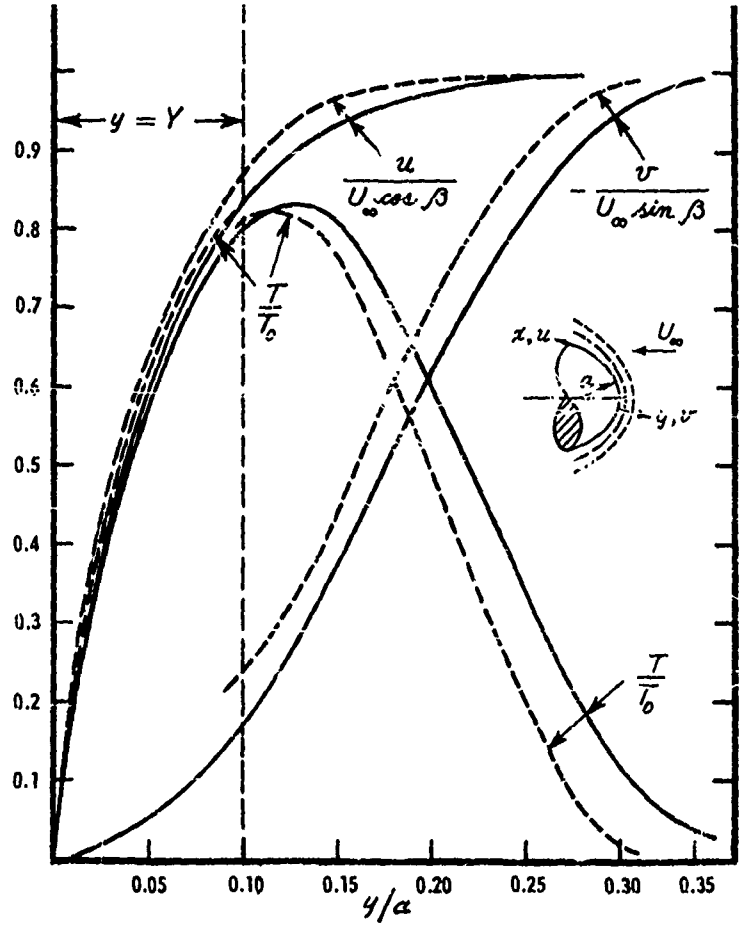
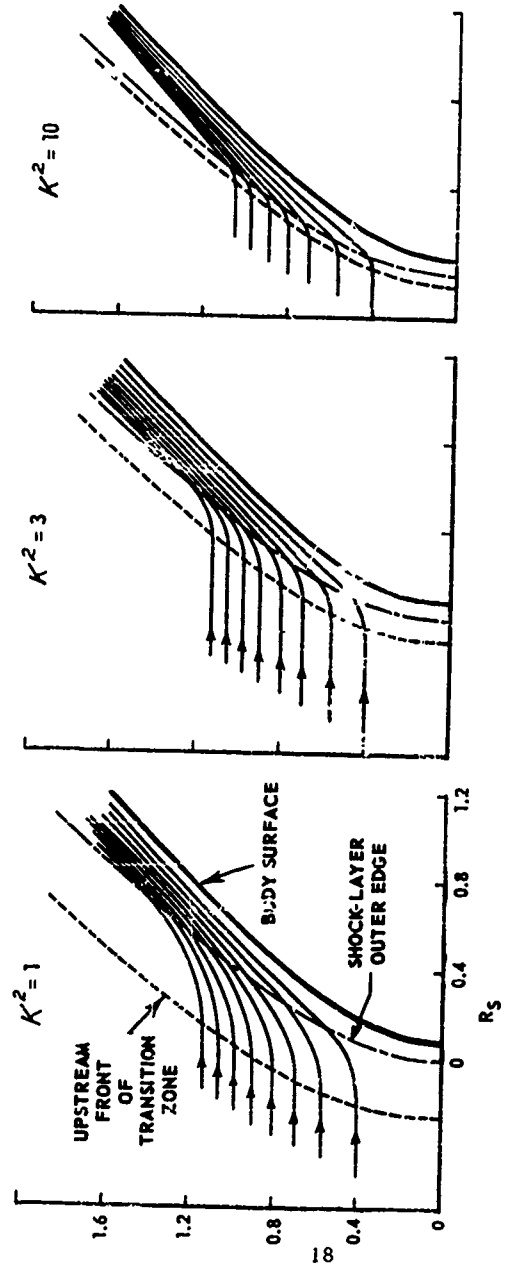


Figure 2 COMPARISON OF SOLUTIONS BASED ON THE TWO-LAYER MODEL OF LEVINSKY AND YOSHIHARA FOR THE STAGNATION REGION AT $Re_b = 25$. NOTE $\gamma = 5/3$.



$\epsilon = 1/8, T_w/T_0 = 1/8, \gamma = 0.71, M_\infty \rightarrow \infty$
 SCALE GIVEN IN TERMS OF R_s

Figure 3 SHOCK TRANSITION ZONE AND STREAMLINE PATTERN AROUND A BODY OF HYPERBOLOIDAL SHAPE FOR SUCCESSIVE DEGREES OF RAREFACTION ($K^2 = 1, 3, \text{ AND } 10$).

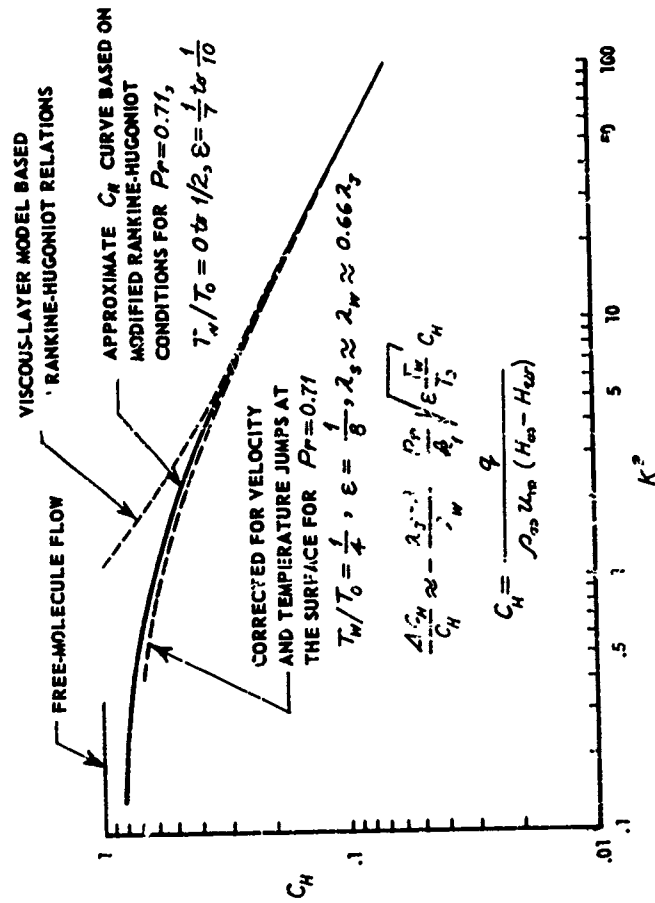


Figure 4 EFFECT OF SLIP AND TEMPERATURE JUMP ON STAGNATION-POINT
 HEAT-TRANSFER RATE AT HIGH AND LOW REYNOLDS NUMBERS.
 NOTE λ_j AND λ_w USED IN THE CALCULATION CORRESPOND TO
 NEARLY UNIT COEFFICIENTS FOR TANGENTIAL MOMENTUM AND
 ENERGY ACCOMMODATIONS.

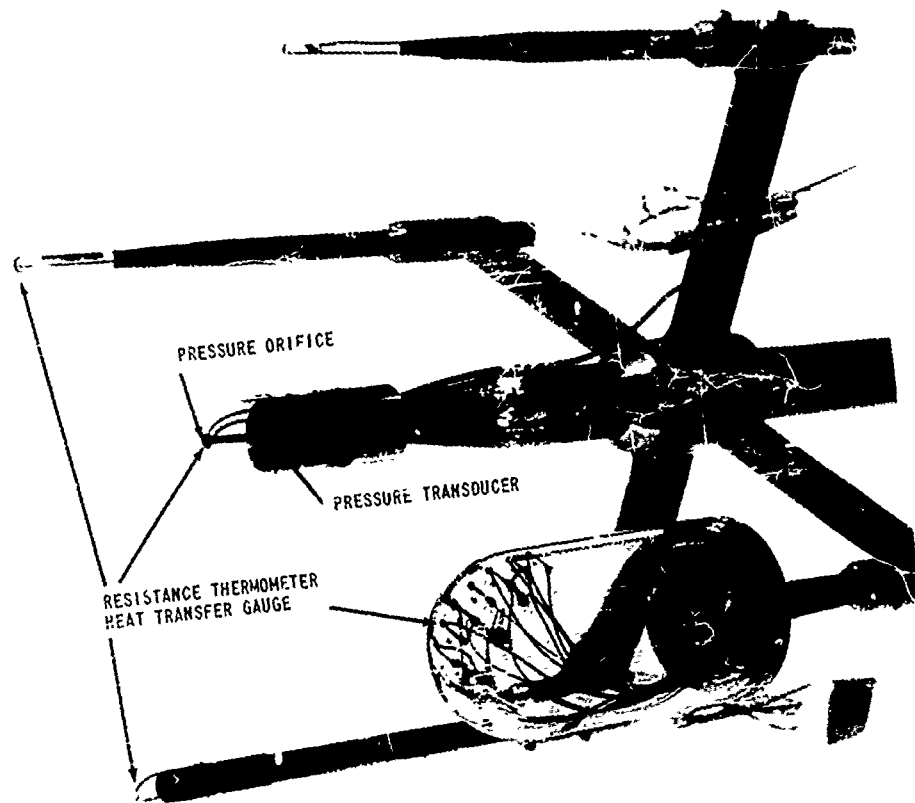


Figure 5 HEMISPHERE-CYLINDER HEAT TRANSFER MODELS

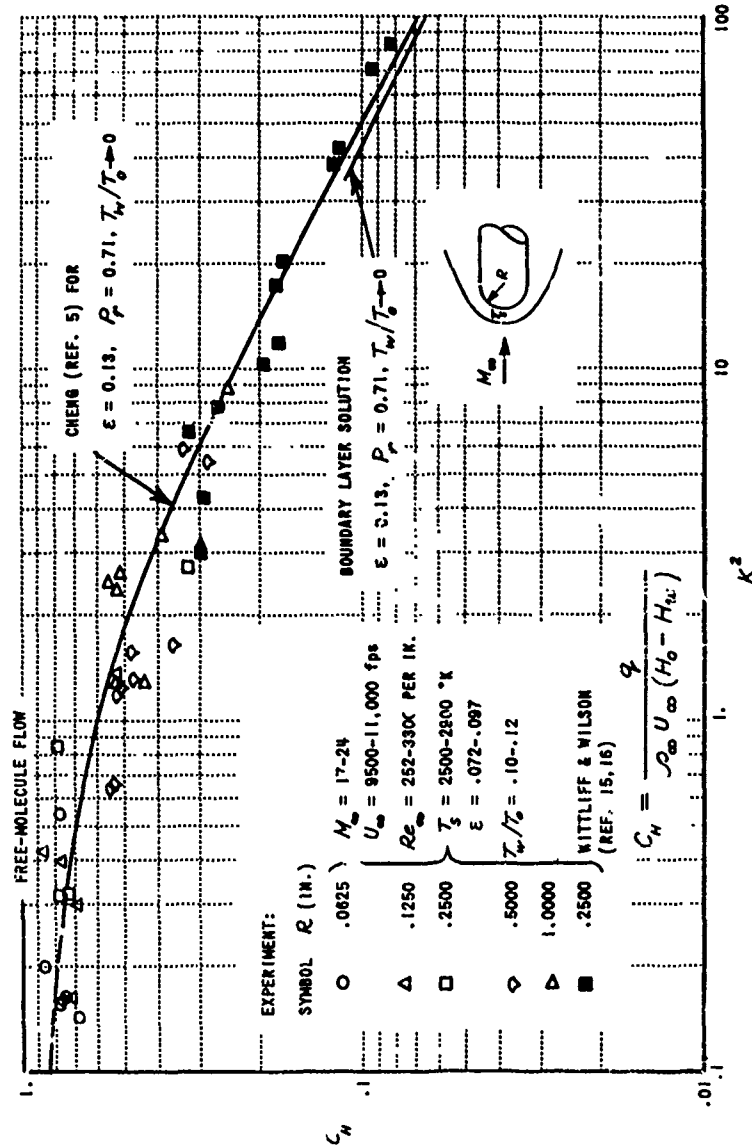


Figure 6 COMPARISON OF THEORY AND EXPERIMENT FOR AXISYMMETRIC STATION-POINT HEAT TRANSFER AT LOW REYNOLDS NUMBERS

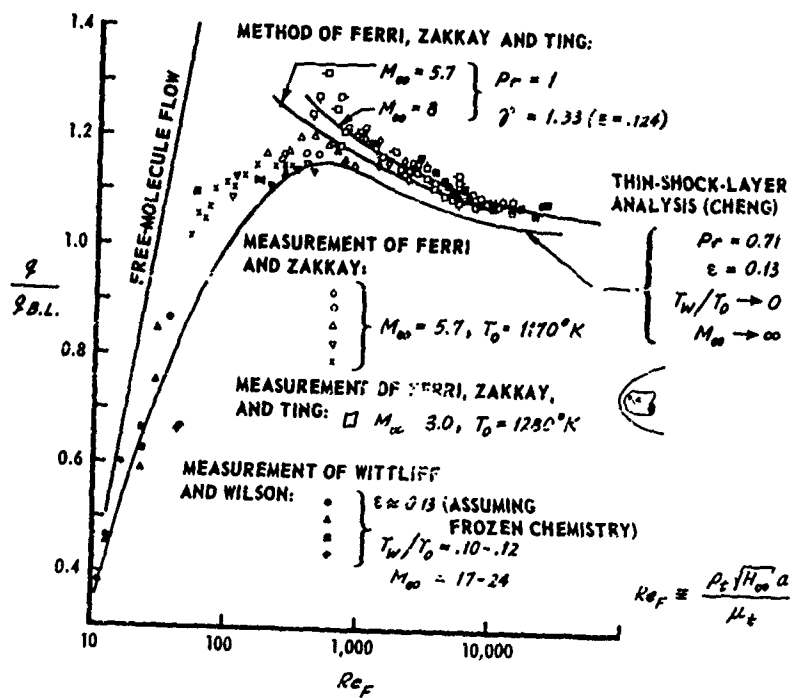


Figure 7 COMPARISON OF STAGNATION-POINT HEAT-TRANSFER MEASUREMENTS ON SPHERICAL BODIES WITH THEORIES

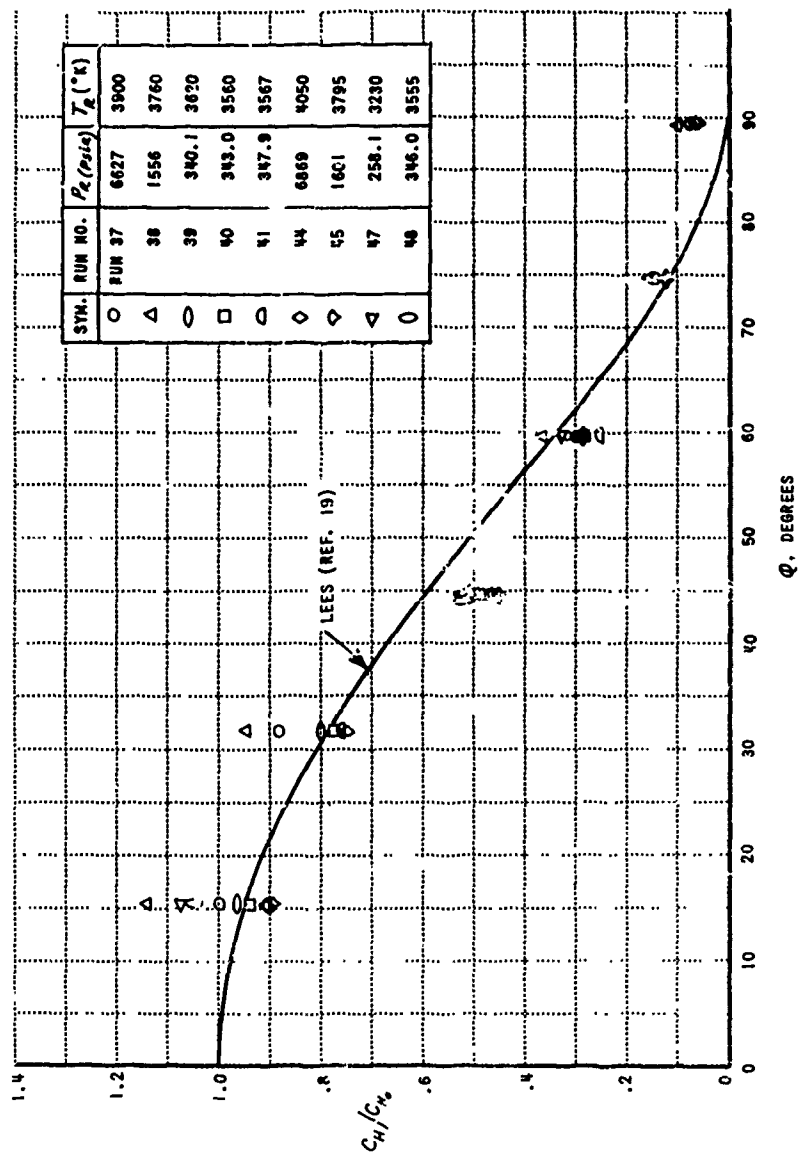


Figure 6 HEAT TRANSFER DISTRIBUTION AROUND AN AXISYMMETRIC BODY
(HEMISPHERE-CYLINDER)

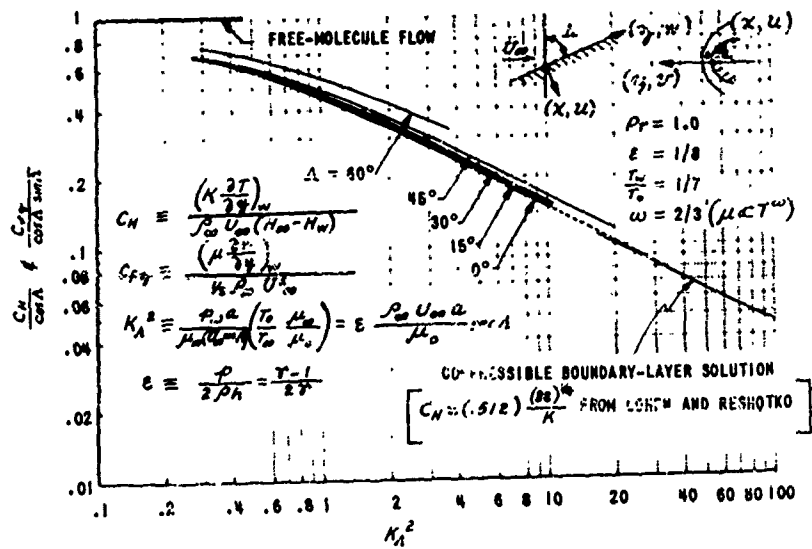


Figure 9 STAGNATION STREAMLINE HEAT-TRANSFER AND SKIN-FRICTION CHARACTERISTICS OF A SWEEPED LEADING EDGE AT VARIOUS DEGREES OF SWEEP AND GAS RAREFACTION

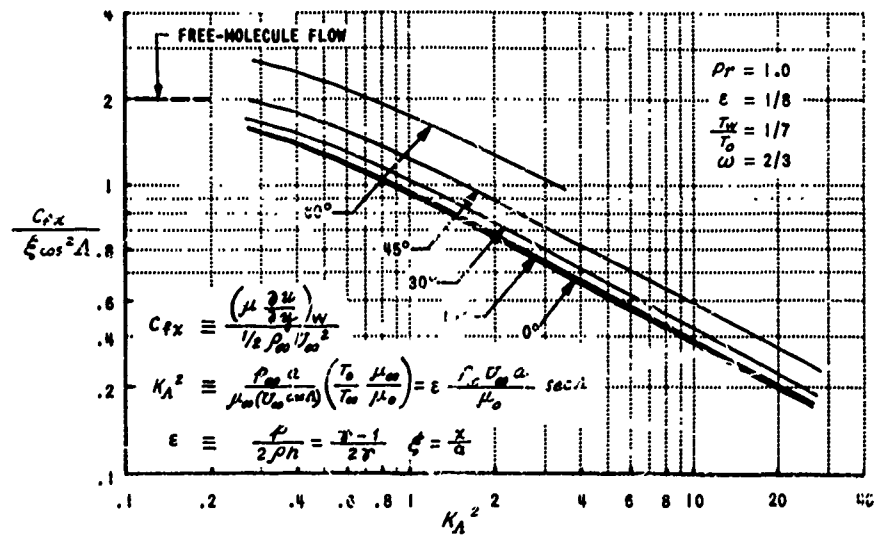


Figure 10 RATE OF INCREASE OF THE CHORDWISE SURFACE STRESS AT THE LEADING EDGE AT VARIOUS DEGREES OF SWEEP AND GAS RAREFACTION

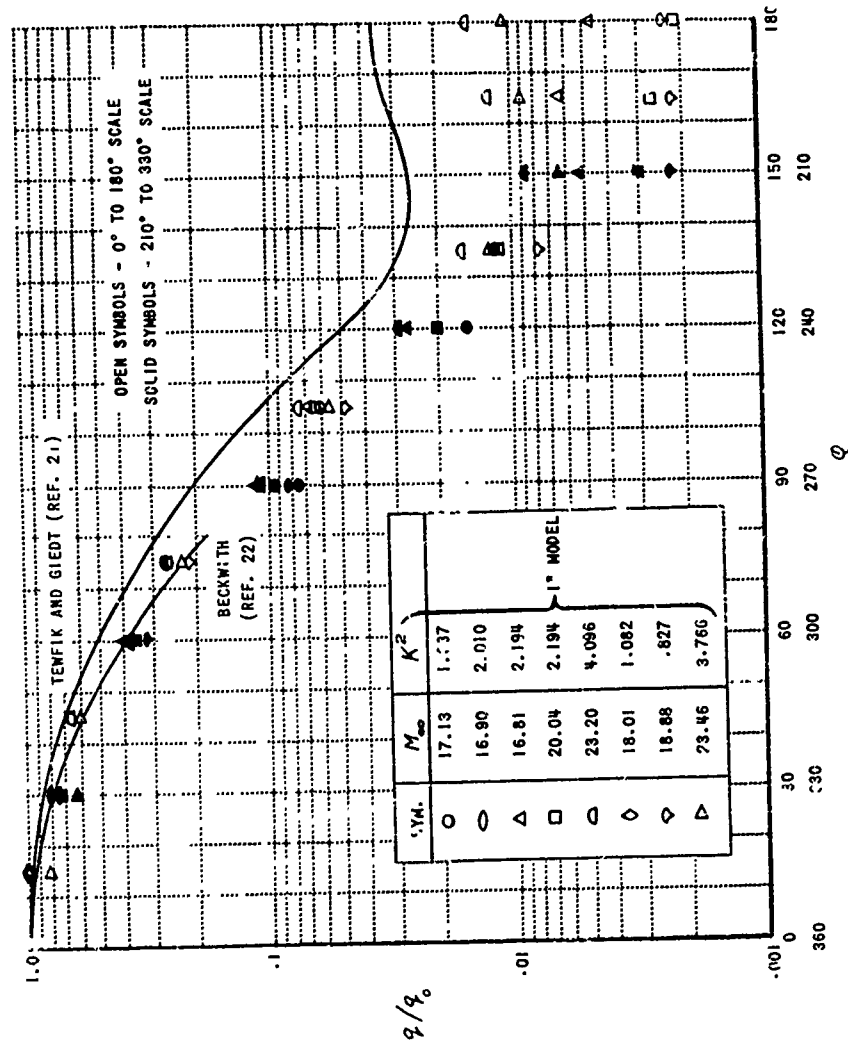


Figure 12 CIRCUMFERENTIAL HEAT TRANSFER ON CYLINDER AT ZERO YAW

q/q_0

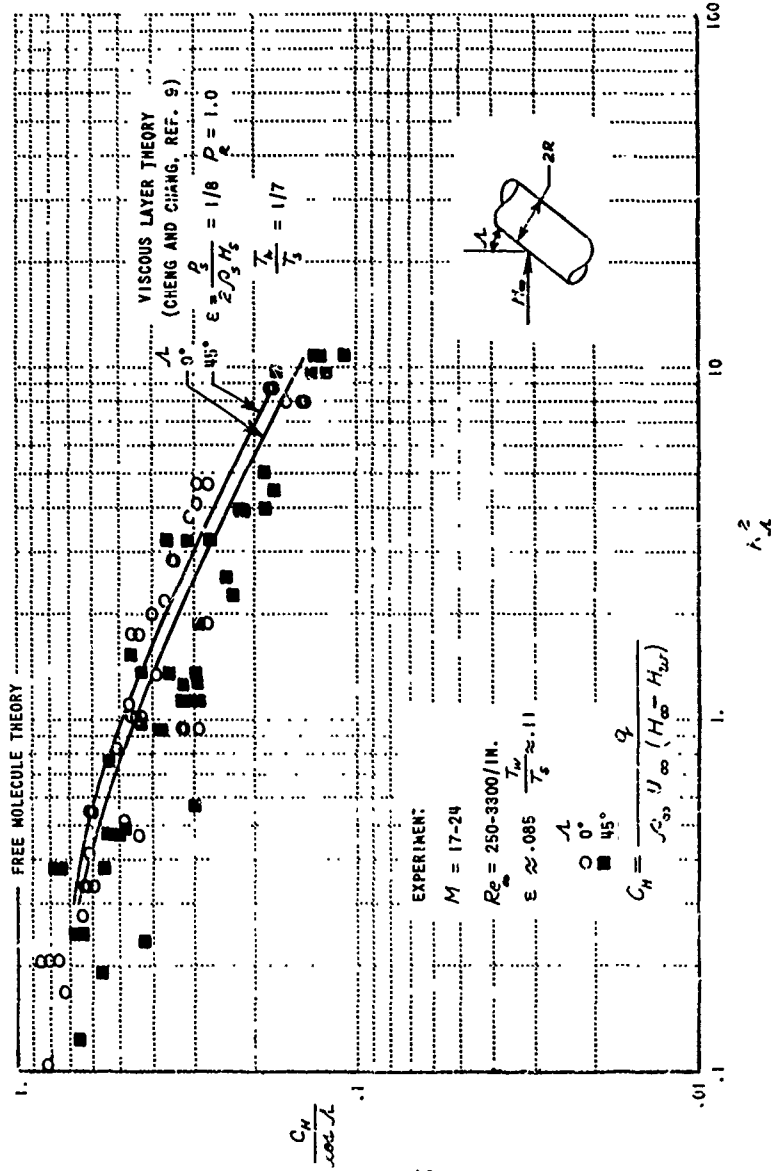
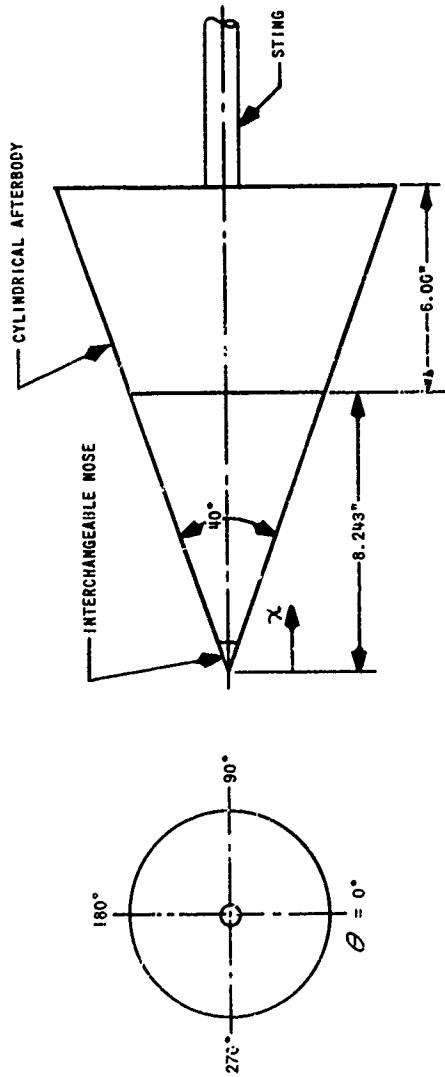


Figure 13 COMPARISON OF THEORY AND EXPERIMENT FOR STAGNATION LINE HEAT TRANSFER TO YAWED CYLINDERS AT LOW REYNOLDS NUMBER



INSTRUMENTED POSITIONS: P = PRESSURE T = TEMPERATURE (HEAT TRANSFER)

χ STA.	$\theta = 0^\circ$	30°	60°	90°	120°	151°	180°	210°	240°	270°	300°	330°
1.060	T						P					
1.650	T						P					
2.882	T			T			P			P		
4.950	T	T	P	T	P	T	P	P	T	P	T	P
7.425	T			T			P			P		

Figure 14 LOCATION OF HEAT TRANSFER GAUGES AND PRESSURE TRANSDUCERS ON THE 40° CONE MODEL



3042

Figure 15 40° CONICAL BODY

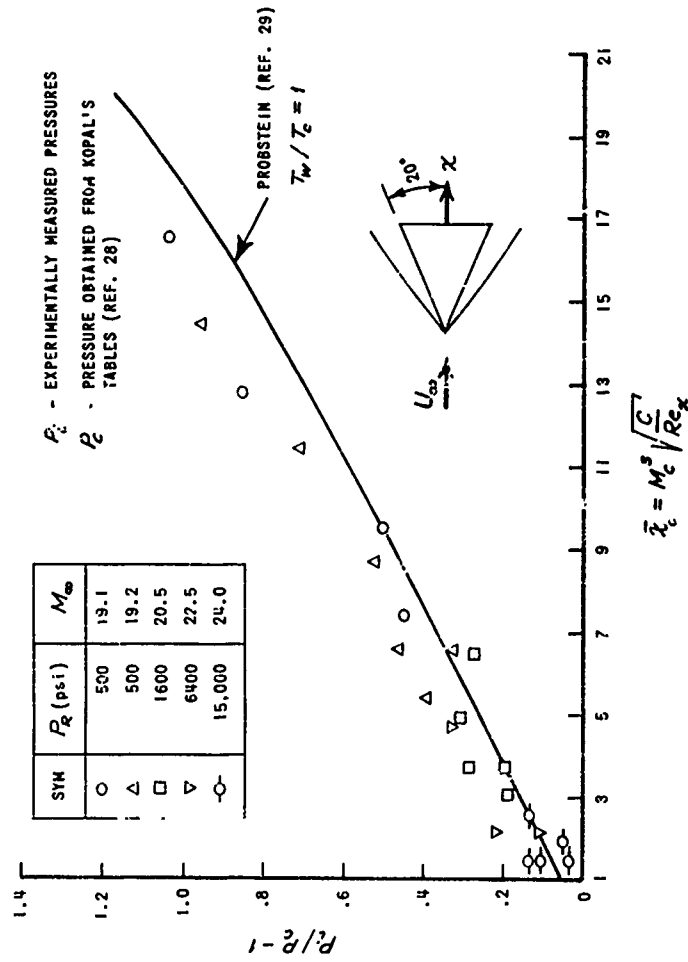


Figure 16 COMPARISON OF PRESSURE RISE ON A 20° HALF ANGLE CONE AT ZERO YAW WITH A BOUNDARY LAYER DISPLACEMENT THEORY

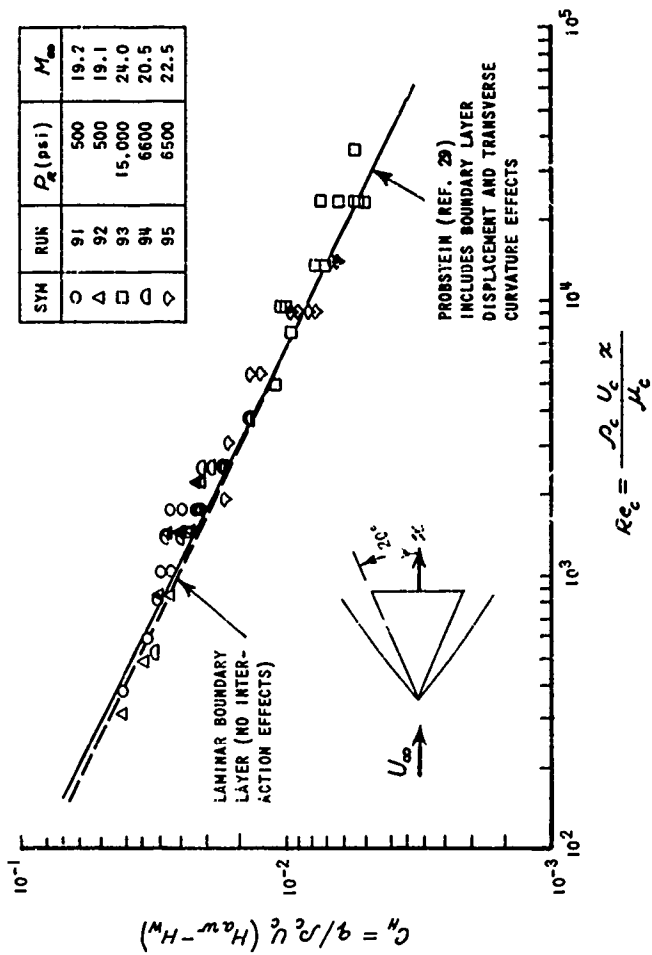


Figure 17 COMPARISON OF HEAT TRANSFER (C_H) WITH LOCAL REYNOLDS NUMBER FOR A 20° HALF ANGLE CONE AT ZERO YAW WITH THEORY

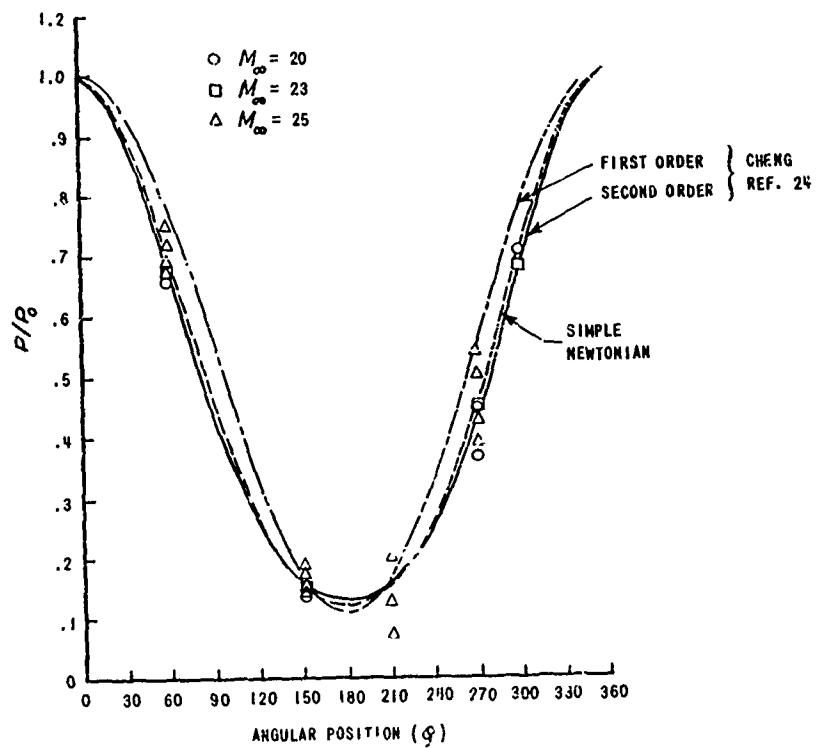


Figure 18 COMPARISON OF CIRCUMFERENTIAL PRESSURE DISTRIBUTION (RELATIVE TO STAGNATION LINE) (P/P_0) FOR A 20° HALF ANGLE CONE AT 10° YAW WITH THEORETICAL PREDICTIONS

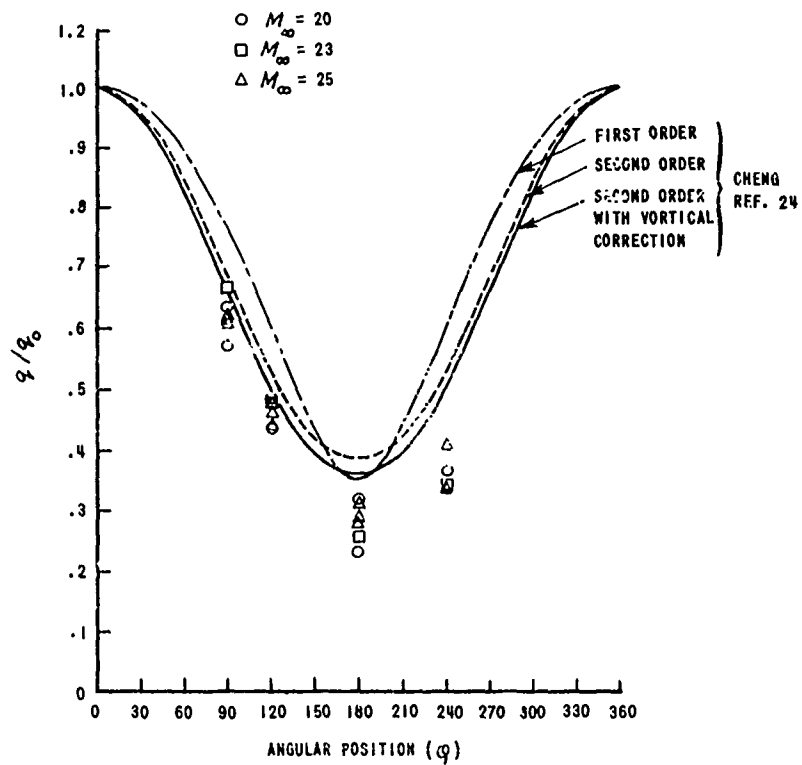


Figure 19 COMPARISON OF CIRCUMFERENTIAL HEAT TRANSFER DISTRIBUTION (RELATIVE TO STAGNATION LINE) (q/q_0) FOR A 20° HALF ANGLE CONE AT 10° YAW WITH THEORETICAL PREDICTIONS